European Journal of Neuroscience, Vol. 6, pp. 640–645

Voltage-dependent Kinetics of *N*-Methyl-D-aspartate Synaptic Currents in Rat Cerebellar Granule Cells

Egidio D'Angelo, Paola Rossi and Vanni Taglietti
Institute of General Physiology, University of Pavia, Via Forlanini 6, 27100 Pavia, Italy

Key words: brain slices, cerebellum, glutamate, patch-clamp, receptors

Abstract

Decay kinetics of *N*-methyl-D-aspartate excitatory postsynaptic currents (NMDA-EPSCs) have been voltage-dependent in some, but not all neurons studied so far, and almost no information has been available on the voltage-dependence of the rising phase. In this work we investigated the effect of membrane potential on rising and decay kinetics of the NMDA-EPSC in cerebellar granule cells using the tight-seal whole-cell recording technique. NMDA-EPSCs were evoked by electrical mossy fibre stimulation in the presence of 10 μM 6-cyano-7-nitroquinoxaline-2,3-dione, 1.2 mM Mg^{2+} and 5 μM glycine. The rate of rise of NMDA-EPSCs remained substantially unchanged when the cell was depolarized, indicating that the limiting step of channel opening was voltage-insensitive. The NMDA-EPSC, however, flattened around the peak and the time-to-peak increased. This observation was explained by the influence of decay. Decay was biphasic and slowed down with membrane depolarization. Moreover, the fast component of decay increased less than the slow component. This complex voltage-dependence may extend the integrative role of the NMDA current during synaptic transmission.

Introduction

The *N*-methyl-D-aspartate (NMDA) subtype of the glutamate receptor is a ligand-gated ion channel that is permeable to monovalent cations and Ca^{2+} (MacDermott *et al.*, 1986; Mayer and Westbrook, 1987; Jahr and Stevens, 1987; Ascher and Nowak, 1988; Iino *et al.*, 1990) and that is blocked by Mg^{2+} in a voltage-dependent manner (Mayer *et al.*, 1984; Nowak *et al.*, 1984). Synaptic activation of NMDA receptors is an important step for the induction of long-term potentiation, an attractive model for learning at the cellular level (Bliss and Collingridge, 1993), and is involved in basic plastic processes including neuronal growth, structuring and death (Meldrum and Garthwaite, 1990; McDonald and Johnston, 1990). Molecular cloning has recently shown that protein subunits constitute hetero-oligomeric NMDA receptors which differ as to their regulatory properties and are unevenly expressed in different brain areas and during development (Moriyoshi *et al.*, 1991; Kutsuwada *et al.*, 1992; Meguro *et al.*, 1992; Monyer *et al.*, 1992; Pollard *et al.*, 1993).

NMDA receptor-mediated excitatory postsynaptic current (NMDA-EPSC) kinetics were several times slower than those of currents produced by non-NMDA and acetylcholine receptors (Forsythe and Westbrook, 1988; Hestrin *et al.*, 1990a,b). However, differences existed between neurons. Decay was biphasic and voltage-dependent in some neurons, such as hippocampal granule cells (Konnerth *et al.*, 1990; Keller *et al.*, 1991), while it was monophasic and voltage-independent in hippocampal pyramidal cells (Hestrin *et al.*, 1990a,c). Additionally, no information was available concerning the voltage-sensitivity of NMDA-EPSC rising phase, which in turn is related to the step(s) leading to channel opening.

In the present work we studied the NMDA-EPSC rising and decay phase in cerebellar granule cells. We found that the rising rate was voltage-insensitive. The decay phase had two components, which differed markedly as to their voltage-sensitivity.

Materials and methods

Slices

Slices of cerebellar vermis 300 μm thick were obtained from rats (Wistar strain) aged from 12 to 16 days, following the procedure described previously (D'Angelo *et al.*, 1990, 1993). The recording chamber was perfused with oxygenated Krebs extracellular solution at a flow rate of 2–3 ml/min and maintained at 27–30°C.

Solutions and drugs

The Krebs extracellular medium had the following composition (mM): NaCl 120, KCl 2, $MgSO_4 \cdot 7H_2O$ 1.2, $NaHCO_3$ 26, KH_2PO_4 1.2, $CaCl_2$ 2 and glucose 11, and it was equilibrated with 95% O_2–5% CO_2 (pH 7.4). Glycine (5 μM) was added to saturate the NMDA receptor binding site (Johnson and Ascher, 1987), and bicuculline

Correspondence to: Dr Egidio D'Angelo, as above

Received 28 June 1993, revised 22 October 1993, accepted 17 November 1993

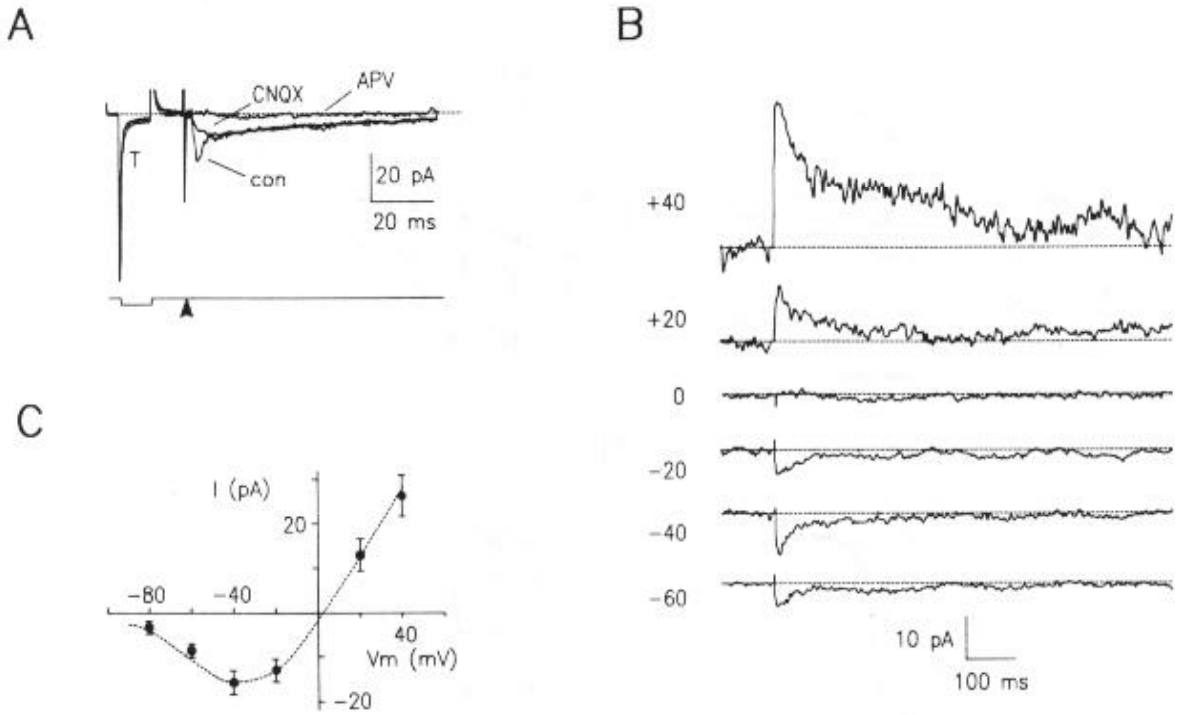

FIG. 1. NMDA synaptic currents in cerebellar granule cells *in situ*. (A) Synaptic currents were recorded in association with a passive current transient ('T'). Averages of 10 traces at −40 mV. Control EPSCs ('con') consisted of a non-NMDA component, which was blocked with 10 μM CNQX ('CNQX'), and an NMDA component, which was inhibited by 50 μM APV ('APV'). The voltage-clamp protocol is indicated below experimental traces. In this and in the other figures current traces were filtered at 0.5 kHz, and the arrowhead indicates mossy fibre stimulation. The stimulus artefact has been partially blanked. (B) NMDA-EPSCs were recorded at different holding potentials, as indicated. NMDA-EPSCs were voltage-dependent in both time-course and peak amplitude. NMDA-EPSC decay (single traces) slowed down with membrane depolarization, while details on the rising phase cannot yet be appreciated on this scale. (C) NMDA-EPSC amplitude showed the characteristic negative slope conductance below −40 mV. The I−V plot was obtained from six cells. The dashed line was drawn by eye through the points.

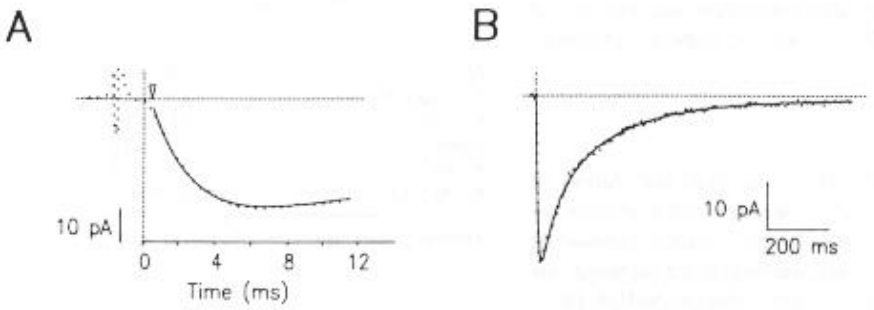

FIG. 2. Time-course of NMDA-EPSCs. (A) NMDA-EPSC rose with a sigmoidal time-course (holding potential = −40 mV; average of 10 traces). The vertical and horizontal dashed lines intersect at the starting point. RT_{10-90} = 4.2 ms, ttp = 6.8 ms, τ_r = 2.4 ms. Equation (1) has been fitted to the points (continuous line). (B) Fitting of equation (1) (continuous line) to an NMDA-EPSC [holding potential = −40 mV; average of 10 traces, a different cell than in (A)]. A_r = 47.4 pA, τ_r = 3.4 ms; A_f = −20.4 pA, τ_f = 53.6 ms; A_s = −27 pA, τ_s = 216 ms ($R > 0.99$).

10 μM (Sigma) to block the inhibitory Golgi cell inputs. The specific non-NMDA and NMDA receptor antagonists 6-cyano-7-nitroquinoxaline-1,3-dione (CNQX) and D-2-amino-5-phosphonovalerate (APV; Tocris Neuramin) were added to the perfusion solution at the final concentration of 10 and 50 μM, respectively. The intracellular solution contained (mM): Cs_2SO_4 62.5, CsCl 20, NaCl 4, EGTA 5, $CaCl_2$ 0.5, HEPES 5, glucose 15, $MgCl_2$ 2 and ATP 3 (pH 7.2 with CsOH).

Stimulation and recording

Afferent fibres were stimulated with a bipolar tungsten electrode (tip diameter = 50 μm; Clark Instruments). Whole-cell recordings were made by standard methods (Hamill *et al.*, 1981; Blanton *et al.*, 1989; Edwards *et al.*, 1989) on granule cells patched in the inner granular layer (D'Angelo *et al.*, 1993). Patch pipettes were pulled from thick-walled borosilicate glass capillaries (Hingelberg); impedance before seal formation was 8−11 MΩ. Whole-cell EPSC recordings were made with an Axopatch-1D (Axon Instruments) patch-clamp amplifier at an output bandwidth of 10 kHz. Each EPSC recording was preceded by a current transient elicited by a 5mV hyperpolarizing voltage step (see Fig. 1A). These passive current transients were used to monitor the stability of recording conditions throughout the experiment and to estimate the electrode series resistance (20−30 MΩ) and membrane capacitance (3−4 pF) (Cull-Candy *et al.*, 1988; Silver *et al.*, 1992;

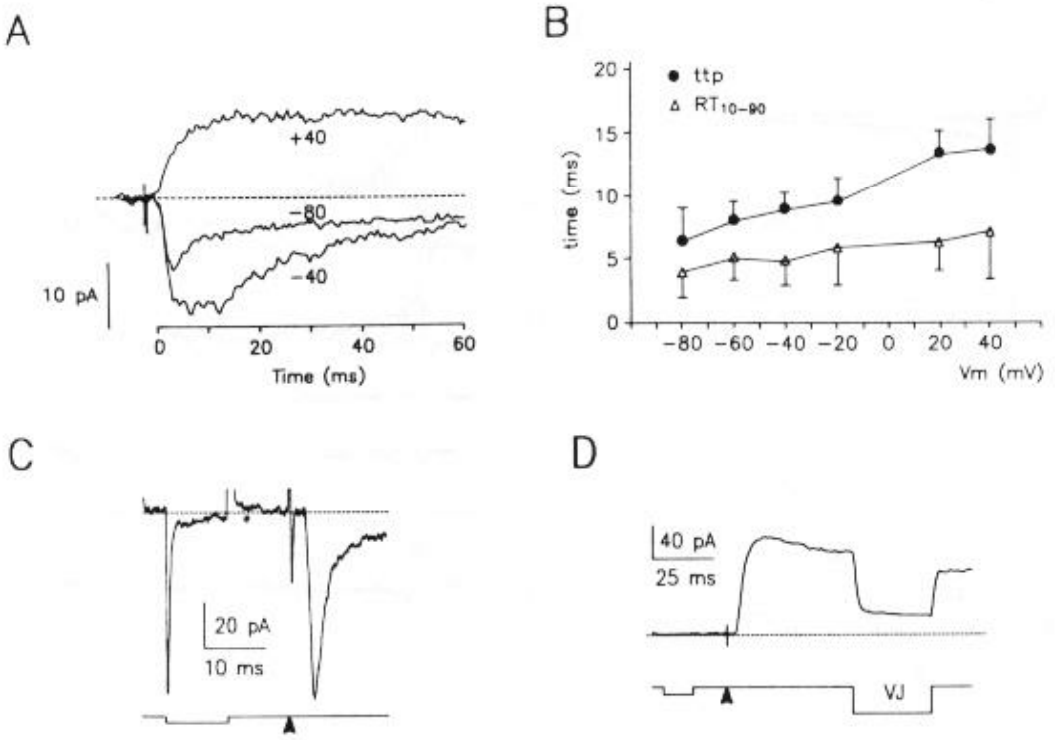

FIG. 3. Voltage-dependence of NMDA-EPSC rising phase. (A) Rising phase of NMDA-EPSCs at different holding potentials (averages of 10 traces). (B) Plots of ttp (dots) and RT_{10-90} (triangles) as a function of holding potential ($n = 5-6$, $n = 3$ at -80 mV). (C) Single non-NMDA current isolated at -100 mV before CNQX application. RT_{10-90} was 710 μs. The voltage-clamp protocol is shown at the bottom. (D) A voltage-jump from +40 mV to 0 mV starting 50 ms after synaptic activation ('VJ' in the voltage-clamp protocol, bottom trace) switched-on Mg^{2+} block with an exponential time constant of 1.1 ms. The current was obtained after leakage subtraction (averages of 10 traces), which also caused the cancellation of the current transient.

D'Angelo *et al.*, 1993). Recordings were made of 4–20 EPSCs at different holding potentials. Current traces were simultaneously stored on a DAT recorder (Biologic DTR-1201) and fed to the mass memory of a PC.

EPSC analysis

The following procedures proved useful to facilitate the analysis of NMDA-EPSCs. A 50 kHz sampling rate was adopted to digitize the passive current transients and part of the synaptic response (including the rising phase of the NMDA current); afterwards the sampling rate was reduced to 4 kHz to digitize the slow and prolonged NMDA-EPSC decay. Digital current traces were played back to exclude anomalous signals and failures, and traces were aligned at the stimulus artefact to obtain average EPSCs. NMDA-EPSCs were digitally filtered at 0.5–1 kHz (−3 dB, simple RC filter) before being analysed. To reduce the contribution of random noise to the measurement of peak position, a three-point smoothing routine was adopted. The starting point was located where the current rose over the baseline (calculated using 50 points before the stimulus artefact), at the beginning of a brief slow-rising convex edge (see Fig. 2A).

EPSC fitting

The time-course of NMDA-EPSCs fitted reliably to the sum of one rising and two decaying exponential functions (see Fig. 2A and B) according to the equation

$$Y(t) = \Sigma_{i=r,f,s} [A_i \cdot (1-\exp^{-t/\tau_i})] \qquad (1)$$

TABLE 1. Kinetic parameters of NMDA-EPSCs at −40 and +40 mV ($n = 9$)

	−40 mV	+40 mV
ttp (ms)	8.8 ±0.3	12.2 ±0.7*
RT_{10-90} (ms)	4.9 ±1	5.1 ±1
τ_r (ms)	3.08 ± 1.1	2.75 ± 0.6
τ_f (ms)	39 ±14	84 ±22*
τ_s (ms)	123 ±24	582 ±271*
$A_f/(A_f+A_s)$	0.64 ± 0.1	0.39 ± 0.2*

Asterisks indicate significant difference ($P < 0.01$).

where A_i are amplitudes ($\Sigma A_i = 0$) and τ_i time constants. The indices r, f and s indicate the rising, the fast decay and the slow decay exponential term, respectively. To improve fittings the convex edge at the beginning of the current was neglected, and the zero-time point was reset accordingly. In some cases the decay phase was fitted to the sum of two exponential functions beginning after current peak, yielding τ_f and τ_s values close to those obtained using equation (1). Equation (1) had no mechanistic implications in our model. Nevertheless it proved useful to predict the influence of decay on the rising phase of EPSCs.

Unless stated otherwise, data were reported as mean ± SEM. Statistical comparisons were made using Student's t-test.

Results

EPSCs were recorded in whole-cell patch-clamp configuration from 14 granule cells in the inner granular layer of rat cerebellar slices, where granule cells receive their excitatory input from mossy fibres (see Ito, 1984).

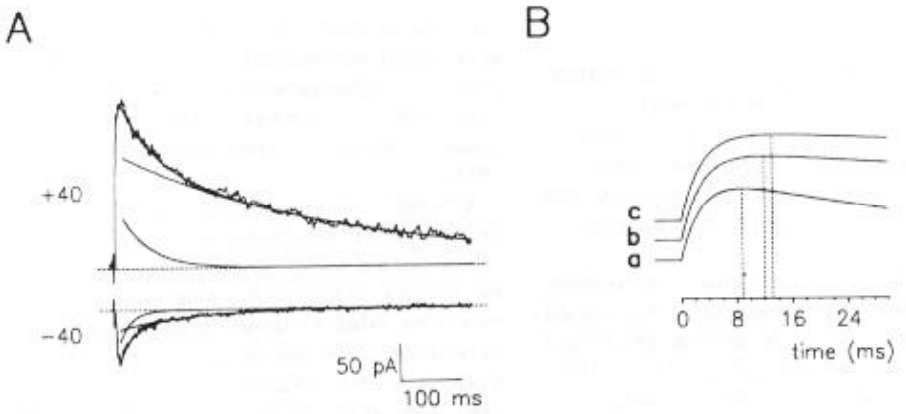

FIG. 4. Voltage-dependence of NMDA-EPSC decay and its influence on the rising phase. (A) Example of bi-exponential fitting of NMDA-EPSC decay (averages of 10 traces): at −40 mV, A_f = −43.3 pA, τ_f = 19.3 ms; A_s = −26.9 pA, τ_s = 111.8 ms (R = 0.99); at +40 mV, A_f = 66.3 pA, τ_f = 49.7 ms; A_s = 147.6 pA, τ_s = 374 ms ($R > 0.99$). Note the different proportion of individual exponential components at the two holding potentials. (B) Simulation of NMDA-EPSC rising phase by changing the decay rate and the relative amplitude of the decay components with constant rising rate. (a) Simulated NMDA-EPSC at −40 mV: rounded values of τ_r, τ_f, τ_s and $A_f/(A_f+A_s)$ were taken from Table 1. Measured parameters: ttp = 8.8 ms, RT_{10-90} = 5.5 ms. (b) When τ_f and τ_s, but not $A_f/(A_f+A_s)$, were updated to their actual values at +40 mV, measured parameters were: ttp = 11.8 ms, RT_{10-90} = 6.4 ms. (c) Together with τ_f and τ_s, $A_f/(A_f+A_s)$ has also been updated to its actual value at +40 mV. Measured parameters: ttp = 13 ms, RT_{10-90} = 6.8 ms.

General features of the NMDA-EPSC

Synaptic currents were composed of non-NMDA and NMDA currents which could be blocked by the selective receptor antagonists CNQX (10 μM) and APV (50 μM), respectively (Fig. 1A). NMDA-EPSCs were recorded at different holding potentials (Fig. 1B). Current−voltage plots for peak amplitude showed a negative slope conductance at holding potentials more negative than −40 mV and reversed close to zero (Fig. 1C). Moreover, NMDA-EPSCs apparently slowed down with membrane depolarization, as was observed in previous studies in cerebellar (D'Angelo *et al.*, 1993) and hippocampal granule cells (Konnerth *et al.*, 1990; Keller *et al.*, 1991). In order to investigate the voltage-dependence of NMDA-EPSCs in detail, we reproduced at first fittings of EPSC time course (Fig. 2).

The NMDA-EPSC arose from the base-line 1−2 ms after stimulus artefact (Fig. 2A). In eight out of 14 cells the rising phase of NMDA-EPSCs was sigmoidal, the initial convex edge usually lasting less than 1 ms. When the edge of the rising phase was excluded, the whole NMDA-EPSC time-course was well approximated as the sum of one growing and two decaying exponentials (Fig. 2B; see equation (1) in Materials and methods).

Kinetics of NMDA-EPSC rising phase

NMDA-EPSCs flattened around peak during membrane depolarization (Fig. 3A). Figure 3B shows a constant increase of time-to-peak (ttp) as a function of holding potential (circles), while rise-time from 10 to 90% of peak amplitude (RT_{10-90}) increased to a lesser extent (triangles). The greater increase of ttp as compared with RT_{10-90} was related to the marked curve flattening occurring after the initial phase of growth. Mean values of ttp and RT_{10-90} at −40 mV and +40 mV are summarized in Table 1. The prolongation of ttp and flattening in the peak region may be related to a simultaneous reduction of the NMDA-EPSC rising rate. Curve fittings, however, indicated that the time constant, τ_r, which is inversely related to the rising rate, did not change significantly with membrane depolarization (Table 1).

A major problem with synaptic current recordings is poor space-clamp on extended dendritic trees. NMDA-EPSCs were much slower than passive current transients (see Fig. 1A) and cerebellar granule cells are electrotonically compact (Silver *et al.*, 1992; D'Angelo *et al.*, 1993), nevertheless currents generated by fast conductance changes occurring at the synapse were monitored to exclude effects of dendritic filtering on the measure of NMDA-EPSC rising rate. Non-NMDA currents were recorded before CNQX application having RT_{10-90} of 0.3−0.9 ms (Fig. 3C). After 10 μM CNQX application, we monitored the on/off-rate of Mg^{2+}-block in NMDA currents (Fig. 3D) during a voltage-jump (Hestrin *et al.*, 1990; Hestrin, 1992). Fitting of the transient generated by the voltage-jump gave a time constant of 0.6−1.8 ms for the on-reaction (see Mayer and Westbrook, 1985). These synaptic currents were indeed much faster than the NMDA-EPSC rising rate, in agreement with previous results.

Kinetics of NMDA-EPSC decay

As shown in Figures 1B and 4A, decay kinetics were apparently voltage-dependent. Decay time courses showed large variability, mostly regarding the slower component at positive membrane potentials. For this reason we compared current decays at −40 mV and +40 mV where signal-to-noise ratio was more favourable (Table 1). Values of τ_f and τ_s at negative potentials differed significantly from those at positive potentials at the 0.01 probability level. Moreover, the relative amplitude of the fast exponential term, $A_f/(A_f+A_s)$, was about twice as large at negative membrane potentials as at positive ones. This result was independent of the fitting procedure, since bi-exponential fitting and fitting using equation (1) were similar.

The influence of decay kinetics on the rising phase

The possible influence of decay kinetics on ttp was then considered. Simulation of the NMDA-EPSC rising phase using equation (1) and data reported on Table 1 indicated that ~70% of the ttp prolongation from −40 mV to +40 mV was due to the slowing down of decay, and the remaining 30% to the increased proportion of the slow component at positive membrane potentials (Fig. 4B). Decay modifications at positive membrane potentials were associated with a modest increase in relative peak amplitude.

Discussion

In this paper we report a study of the voltage-sensitivity of NMDA-EPSCs in cerebellar granule cells. NMDA-EPSCs showed three main kinetic changes accompanying membrane depolarization: ttp grew longer, the biphasic decay slowed down, and the relative amplitude of the slow decay component increased. Since the rising rate remained virtually unchanged, the changes of EPSC decay were the cause of ttp prolongation.

A voltage-dependent change of ttp has not previously been reported. However, since an increase in ttp with depolarization was caused indirectly by changes of decay kinetics, ttp increase may be detected also in other neurons with voltage-dependent decay (Keller *et al.*, 1991; Carmignoto and Vicini, 1992; Hestrin, 1992). In these neurons, as well as in cerebellar granule cells, monitoring the time-course of non-NMDA currents and Mg^{2+}-block on the NMDA channel excluded the possibility that electrotonic filtering could mask major changes in ttp. Nevertheless, it should be considered that the simple synaptic organization of cerebellar granule cells (Hamori and Somogyi, 1983; D'Angelo *et al.*, 1991, 1993) may enhance resolution of rising and decay kinetics by minimizing time- and space-scattering of synaptic currents (just 1–3 synapses were activated in these experiments, not shown).

Rising rate voltage-independence

Compelling evidence indicates that the synaptic glutamate transient is much shorter than the NMDA-EPSC rising phase (Hestrin *et al.*, 1990c; Lester *et al.*, 1990; Clements *et al.*, 1992). This suggests that the rate-limiting step of the NMDA-EPSC rising phase is located postsynaptically at the channel level, and that information about the process leading to channel opening can be obtained by analysing the rising phase of EPSCs. In the present study we show that the rate-limiting step of NMDA channel opening is voltage-insensitive. It should be noted that information on the states leading to channel opening cannot be easily obtained with single channel recordings in the presence of a steady agonist concentration. Comparative experiments should be obtained by fast perfusion of glutamate on outside-out membrane patches, since this method has been shown to reproduce kinetics comparable to those of NMDA-EPSCs (Lester *et al.*, 1990).

Decay rate voltage-dependence

If biphasic decay were to be explained by co-expression of two NMDA receptor sub-types, as proposed in neurons of the superior colliculus (Hestrin, 1992) and of the visual cortex (Carmignoto and Vicini, 1992), then each decay component would represent the property of a different molecule. After birth NR2A and NR2C cDNA transcripts ascend, substituting NR2B in the cerebellum (Kutsuwada *et al.*, 1992; Monyer *et al.*, 1992; Monyer, 1993; Pollard *et al.*, 1993). Thus, at the age under investigation (P12–P16) both NR2A and NR2C subunits, and still perhaps NR2B at a lower degree, should be expressed in granule cells. It should be noted that during this time-window the NMDA component of EPSCs slightly increased in size without remarkable changes of decay kinetics and Mg^{2+} sensitivity (D'Angelo *et al.*, 1993), suggesting that no major changes are occurring at the molecular level.

It is tempting to speculate that the lower voltage-sensitivity of the faster decay component is explained by the lower Mg^{2+} sensitivity of NR1-NR2C relative to NR1-NR2A/NR1-NR2B channel currents (Monyer *et al.*, 1992; Kutsuwada *et al.*, 1992). In a preceding study we indeed observed that voltage-sensitivity of NMDA-EPSC decay was reduced after virtual removal of extracellular Mg^{2+} (D'Angelo *et al.*, 1993), but residual voltage-sensitivity made further distinction of the Mg^{2+} effect between the two components uncertain (see Keller *et al.*, 1991). Differences in Mg^{2+}-block were observed between immature and mature hippocampal pyramidal cells (Ben-Ari *et al.*, 1988).

Although the dual-channel hypothesis is supported by the demonstration of two channel subunits in postnatal rat cerebellum, bi-exponential and voltage-sensitive decay kinetics could also be produced by complex modality of gating within a homogeneous channel population. NMDA channel openings organized in complex clusters of bursts have been demonstrated in cerebellar granule cells (Gibb and Colquhoun, 1991, 1992; Howe *et al.*, 1991; Edmonds and Colquhoun, 1992; Stern *et al.*, 1992), although the effects of Mg^{2+} and voltage are still unknown. Further study is required, therefore, to understand the molecular nature of NMDA-EPSC kinetics in cerebellar granule cells.

Functional implications

Functionally, regional and development differences of NMDA-EPSC voltage-dependence may underlie different requirements for synaptic encoding. The strongly voltage-dependent time-course in the peak region, and the increase of the slower component observed here are suited to amplify the effect of NMDA receptor activation. While fast inactivation will occur with modest synaptic depolarization, a strong depolarization (e.g. during high frequency synaptic activation) will make the NMDA conductance remain high for longer, extending temporal integration to lower input frequencies (see Fig. 3A). The simultaneous reduction of Mg^{2+} block will enhance this effect by increasing the current flowing through the NMDA channel. Therefore, the combination of kinetic and conductance changes allows a sudden switching on of the integrative properties of the NMDA system, favouring both temporal summation of excitatory synaptic potentials and repetitive firing. By controlling the extent of Ca^{2+} influx this mechanism may also contribute to the reduction of the potential neurotoxic action of glutamate at rest and to set a trigger level for synaptic plasticity during neuronal activation.

Acknowledgements

This work was supported by grants from MURST and INFM of Italy.

Abbreviations

APV	D-2-amino-5-phosphonovalerate
CNQX	6-cyano-7-nitroquinoxaline-2,3-dione
EPSC	excitatory postsynaptic current
NMDA	*N*-methyl-D-aspartate
RT_{10-90}	10–90% rise-time
ttp	time-to-peak

References

Ascher, P. and Nowak, L. (1988) The role of divalent cations in the *N*-methyl-D-aspartate responses of mouse central neurones in culture. *J. Physiol.*, **399**, 247–266.

Ben-ari, J., Cherubini, E. and Krnjevic, K. (1988) Changes in voltage dependence of NMDA currents during development. *Neurosci. Lett.*, **94**, 88–92.

Blanton, M. G., Lo Turco, J. J. and Kriegstein, A. R. (1989) Whole cell recording from neurons in slices of reptilian and mammalian cerebral cortex. *J. Neurosci. Methods*, **30**, 203–210.

Bliss, T. V. P. and Collingridge, G. L. (1993) A synaptic model for memory: long-term potentiation in the hippocampus. *Nature*, **361**, 31–39.

Carmignoto, G. and Vicini, S. (1992) Activity-dependent decrease in NMDA receptor responses during development of the visual cortex. *Science*, **258**, 1007–1011.

Clements, J. D., Lester, R. A. J., Gang Tong, Jahr, C. E. and Westbrook, G. L. (1992) The time course of glutamate in the synaptic cleft. *Science*, **258**, 1498–1501.

Cull-Candy, S. G., Howe, J. R. and Ogden, D. C. (1988) Noise and single channels activated by excitatory amino acids in rat cerebellar granule cells. *J. Physiol.*, **400**, 189–222.

D'Angelo, E., Rossi, P. and Garthwaite, J. (1990) Dual-component NMDA receptor currents at a single central synapse. *Nature*, **346**, 467–470.

D'Angelo, E., Rossi, P. and Taglietti, V. (1991) Cerebellar granule cells originate similar EPSCs at each one of their excitatory synapses. *Eur. J. Neurosci.*, **4** (Suppl), A2061.

D'Angelo, E., Rossi, P. and Taglietti, V. (1993) Different proportions of NMDA and non-NMDA currents at the mossy fibre–granule cell synapses of developing rat cerebellum. *Neuroscience*, **53**, 121–130.

Edmonds, B. and Colquhoun, D. (1992) Rapid decay of averaged single-channel NMDA receptor activation recorded at low agonist concentration. *Proc. R. Soc. Lond. B*, **250**, 279–286.

Edwards, F. A., Konnerth, A., Sakmann, B. and Takahashi, T. (1989) A thin slice preparation for patch clamp recordings from neurones of the mammalian central nervous system. *Pflüger's Arch.*, **414**, 600–612.

Forsythe, I. D. and Westbrook, G. L. (1988) Slow excitatory postsynaptic currents mediated by *N*-methyl-D-aspartate receptors on cultured mouse central neurones. *J. Physiol.*, **396**, 515–533.

Gibb, A. J. and Colquhoun, D. (1991) Glutamate activation of a single NMDA receptor-channel produces a cluster of channel openings. *Proc. R. Soc. Lond. B*, **243**, 39–45.

Gibb, A. J. and Colquhoun, D. (1992) Activation of *N*-methyl-D-aspartate receptors by L-glutamate in cells dissociated from adult rat hippocampus. *J. Physiol.*, **456**, 143–179.

Hamill, O. P., Marty, A., Neher, E., Sakmann, B. and Sigworth, F. J. (1981) Improved patch-clamp techniques for high-resolution current recording from cells and cell-free membrane patches. *Pflüger's Arch.*, **391**, 85–100.

Hamori, J. and Somogyi, J. (1983) Differentiation of cerebellar mossy fibre synapses in the rat: a quantitative electron microscope study. *J. Comp. Neurol.*, **220**, 365–377.

Hestrin, S. (1992) Developmental regulation of NMDA receptor-mediated synaptic currents at a central synapse. *Nature*, **357**, 686–689.

Hestrin, S., Nicoll, R. A., Perkel, D. J. and Sah, P. (1990a) Analysis of excitatory synaptic action in pyramidal cells using whole cell recordings from rat hippocampal slices. *J. Physiol.*, **422**, 203–225.

Hestrin, S., Perkel, D. J., Sah, P., Manabe, T., Renner, P. and Nicoll, R. A. (1990b) Physiological properties of excitatory synaptic transmission in the central nervous system. *Cold Spring Harbor Symp. Quant. Biol.*, **55**, 87–93.

Hestrin, S., Sah, P. and Nicoll, R. A. (1990c) Mechanisms generating the time course of dual component excitatory synaptic currents recorded in hippocampal slices. *Neuron*, **5**, 237–253.

Howe, J. R., Colquhoun, D. and Cull-Candy, S. G. (1988) On the kinetics of large-conductance glutamate-receptor ion channels in rat cerebellar granule cells. *Proc. R. Soc. Lond. B*, **233**, 407–422.

Howe, J. R., Cull-Candy, S. G. and Colquhoun, D. (1991) Currents through glutamate receptor channels in outside-out patches from rat cerebellar granule cells. *J. Physiol.*, **432**, 143–202.

Iino, M., Ozawa, S. and Tsuzuki, K. (1990) Permeation of calcium through excitatory amino acid receptor channels in cultured rat hippocampal neurones. *J. Physiol.*, **424**, 151–165.

Ito, M. (1984) *The Cerebellum and Neural Control*. Raven Press, New York.

Jahr, C. E. and Stevens, C. F. (1987) Glutamate activates multiple single channel conductances in hippocampal neurones. *Nature*, **325**, 522–525.

Johnson, J. W. and Ascher, P. (1987) Glycine potentiates the NMDA response in cultured mouse brain neurones. *Nature*, **325**, 529–531.

Keller, B. U., Konnerth, A. and Yaari, Y. (1991) Patch clamp analysis of excitatory synaptic currents in granule cells of rat hippocampus. *J. Physiol.*, **435**, 275–293.

Konnerth, A., Keller, B. U., Ballanyi, K. and Yaari, Y. (1990) Voltage sensitivity of NMDA-receptor mediated postsynaptic currents. *Exp. Brain Res.*, **81**, 209–212.

Kutsuwada, T., Kashiwabuchi, N., Mori, H., Sakimura, K., Kushiya, E., Araki, K., Meguro, H., Masaki, H., Kumanishi, T., Arakawa, M. and Mishina, M. (1992) Molecular diversity of the NMDA receptor channel. *Nature*, **358**, 36–41.

Lester, R. A. J., Clements, J. D., Westbrook, G. L. and Jahr, C. E. (1990) Channel kinetics determine the time course of NMDA receptor mediated synaptic currents. *Nature*, **346**, 565–567.

MacDermott, A. B., Mayer, M. L., Westbrook, G. L., Smith, S. J. and Barker, J. L. (1986) NMDA-receptor activation increases cytoplasmic calcium concentration in cultured spinal cord neurones. *Nature*, **321**, 519–522.

Mayer, M. L. and Westbrook, G. L. (1985) The action of *N*-methyl-D-aspartate acid on mouse spinal neurones in culture. *J. Physiol.*, **361**, 65–90.

Mayer, M. L. and Westbrook, G. L. (1987) Permeation and block of *N*-methyl-D-aspartate acid receptor channels by divalent cations in mouse cultured central neurones. *J. Physiol.*, **394**, 501–527.

Mayer, M. L., Westbrook, G. L. and Guthrie, P. B. (1984) Voltage-dependent block by Mg^{2+} of NMDA responses in spinal cord neurones. *Nature*, **309**, 261–263.

McDonald, J. W. and Johnston, M. (1990) Physiological and pathophysiological roles of excitatory amino acids during central nervous system development. *Brain Res. Rev.*, **15**, 41–70.

Meguro, H., Mori, H., Araki, K., Kushiya, E., Kutsuwada, T., Yamazaki, M., Kumanishi, T., Arakawa, M., Sakimura, K. and Mishina, M. (1992) Functional characterization of a heteromeric NMDA receptor channel expressed from cloned cDNAs. *Nature*, **357**, 70–74.

Meldrum, B. and Garthwaite, J. (1990) Excitatory amino acid neurotoxicity and neurodegenerative diseases. *Trends Pharmacol. Sci.*, **11**, 379–387.

Monyer, H. (1993) Developmental expression of four NMDA receptor subtypes. *Eur. J. Neurosci.*, **6** (Suppl.), SY819.

Monyer, H., Sprengel, R., Schoepfer, R., Herb, A., Higuchi, M., Lomeli, H., Burnashev, N., Sackmann, B. and Seeburg, P. H. (1992) Heteromeric NMDA receptors: molecular and functional distinction of subtypes. *Science*, **256**, 1271–1221.

Moriyoshi, K., Masu, M., Ishii, T., Shigemoto, R., Mizuno, N. and Nakanishi, S. (1991) Molecular cloning and characterization of the rat NMDA receptor. *Nature*, **354**, 31–37.

Nowak, L., Bregestovski, P., Ascher, P., Herbet, A. and Prochiantz, A. (1984) Magnesium gates glutamate-activated channels in mouse central neurones. *Nature*, **307**, 462–465.

Pollard, H., Khrestchatisky, M., Moreau, J. and Ben Ari, Y. (1993) Transient expression of the NR2C subunit of the NMDA receptor in developing brain. *NeuroReport*, **4**, 411–414.

Silver, R. A., Traynelis, S. F. and Cull-Candy, S. G. (1992) Rapid-time-course miniature and evoked excitatory currents at cerebellar synapses *in situ*. *Nature*, **355**, 163–166.

Stern, P., Behe, P., Schoepfer, R. and Colquhoun, D. (1992) Single-channel conductances of NMDA receptors expressed from cloned cDNAs: comparison with native receptors. *Proc. R. Soc. Lond. B*, **250**, 271–277.